The American Journal of Pathology, Vol. 171, No. 5, November 2007

DOI: 10.2353/ajpath.2007.070406

Immunopathology and Infectious Disease

Pathogenesis of Aryl Hydrocarbon Receptor-Mediated Development of Lymphoma Is Associated with Increased Cyclooxygenase-2 Expression

Christoph F.A. Vogel,* Wen Li,* Eric Sciullo,* John Newman,† Bruce Hammock,‡ J. Rachel Reader,§ Joseph Tuscano,¶ and Fumio Matsumura*

From the Departments of Environmental Toxicology, and Entomology,‡ the Nutrition Department,† and the Comparative Pathology Laboratory,§ School of Veterinary Medicine, University of California, Davis, Davis; and the Department of Internal Medicine,¶ Division of Hematology and Oncology, Cancer Center, University of California, Sacramento, California*

Epidemiological studies indicate that exposure to environmental pollutants such as pesticides and dioxins leads to the pathogenesis of lymphoma and leukemia. Here, we show that activation of the aryl hydrocarbon receptor (AhR) by 2,3,7,8-tetrachlorodibenzo-*p*-dioxin (TCDD) resulted in loss of the programmed cell death (apoptosis) response in three different lymphoma cell lines, which plays a key role in the development of cancer, especially lymphoma and leukemia. The AhR-mediated inhibition of apoptosis *in vitro* was associated with a clear increase of cyclooxygenase-2 (COX-2) and deregulation of genes of the B-cell lymphoma-2 (Bcl-2) family involved in apoptosis including Bcl-xl and Mcl-1 in several lymphoma cell lines. Treatment with the COX-2 inhibitor NS-398 and the AhR antagonist 3′-methoxy-4′-nitroflavone abolished the TCDD-induced resistance of apoptosis *in vitro*. Furthermore, using micropositron emission tomography imaging, *in vivo* findings demonstrated that exposure to TCDD promotes the development of lymphoma in superficial lymph nodes of C57BL/10J mice, which was associated with a marked increase of COX-2 expression in the affected lymph nodes. The results indicate that AhR activation and COX-2 overexpression likely represent a mechanism of resistance to apoptosis in lymphoma cell lines that might be relevant for the development of lymphoma *in vivo*. *(Am J Pathol 2007, 171:1538–1548; DOI: 10.2353/ajpath.2007.070406)*

Approximately 4.5 million people worldwide are living with various forms of lymphoma, and an estimated 300,000 people die each year from lymphoma. In terms of incidence and death, non-Hodgkin's lymphoma (NHL) is the second fastest growing cancer in the United States and the third fastest growing in the rest of the world. NHL has grown in incidence by 80% since the early 1970s in the United States.[1–3] The etiology of NHL and leukemia is still primarily unknown; however, research has focused on at least four possible factors that may contribute to the development of lymphoma, including genetic factors, autoimmune disorders, viruses such as human immunodeficiency virus, and exposure to pesticides.[4,5] Epidemiological studies have linked exposure to environmental contaminants such as polychlorinated biphenyls and polychlorinated dibenzo-dioxins/furans (PCDD/PCDF) with increased incidence of NHL and myeloid leukemia.[6–13] The environmental pollutant dioxin or 2,3,7,8-tetrachlorodibenzo-*p*-dioxin (TCDD or dioxin) is a byproduct in pesticides and a persistent chemical formed in various combustion processes that accumulates in the food chain. TCDD is now listed as a human carcinogen.[14] TCDD is the prototype of AhR ligands with a very high binding affinity for the AhR. The involvement of an AhR-mediated pathway has been implicated in animal models demonstrating benzene-induced leukemia.[15] Activation of the AhR in the absence of exogenous ligands has been described in T-cell leukemia cells and lymphoma cells.[16,17] A hallmark of leukemic/lymphoma cells is the ability to proliferate in the absence of exogenous growth factors and to escape apoptosis. As a consequence of a suppressed apoptotic response, malignant cells can escape from immune control, accumulate genetic defects, and proliferate to expand their cell population. Therefore, inhibition of DNA damage- or stress-induced apoptosis

Supported by the National Institute of Environmental Health Sciences (grants R01-ES005233 and P30-ES05707) and the American Cancer Society (grant IRG 95-125-07).

Accepted for publication June 29, 2007.

Address reprint requests to Christoph Vogel, Department of Environmental Toxicology, University of California, Davis, One Shields Ave., Davis, CA 95616. E-mail: cfvogel@ucdavis.edu.

plays an important role in the development of lymphoma/leukemia and has been suggested as a mechanism of carcinogenic action of AhR-activating agents like TCDD.[18,19]

Previous studies have shown that the activated AhR may inhibit apoptosis in different cell types and tissue. For instance, the ligand-activated AhR led to resistance of UV-induced apoptosis in rat primary and mouse hepatocytes.[20,21] Ray and Swanson[22] have shown that TCDD induces immortalization and inhibits senescence in normal human keratinocytes in an AhR-dependent manner. Further, the tumor-promoting activity of TCDD was found to be preferentially mediated by a decrease of apoptosis in enzyme-altered liver foci.[23] Recent data obtained by Davis and colleagues[24] and Park and Matsumura[25] show that the TCDD-activated AhR also inhibits apoptosis in the human mammary epithelial cell line MCF10A.

The CAAT/enhancer-binding protein β (C/EBPβ) is implicated in the regulation of many different molecular and physiological processes. Recent studies identified C/EBPβ as a critical component of an autocrine survival pathway in myeloid tumor cells.[26] C/EBPβ has also been shown to deregulate Bcl-2 and apoptosis in lymphoma cells.[27] In addition, overexpression of C/EBPβ leads to hyperproliferation and transformation of normal mammary epithelial MCF10A cells.[28] C/EBPβ knockout mice exhibit increased (17-fold) apoptosis in epidermal keratinocytes in response to carcinogen treatment and are completely resistant to carcinogen-induced skin tumorigenesis compared with wild-type mice[29,30] and seem also to be resistant to development of lymphomas in a carcinogenesis model, whereas wild-type animals frequently developed lymphomas (Dr. Peter Johnson, National Cancer Institute–Frederick; personnel communication).

C/EBPβ has also emerged as a key transactivator for cyclooxygenase (COX)-2 expression induced by proinflammatory mediators. It has been shown to regulate COX-2 transcriptional activation in murine and human cells induced by diverse inflammatory stimuli[31] and chemicals.[32,33] COX-2 is an important enzyme in regulation of cell growth, differentiation, and apoptosis.[34] COX-2 converts arachidonic acid to prostaglandins, which results in up-regulation of antiapoptotic proteins Bcl-2, PI3K-Akt, and Mcl-1, which may lead to enhanced tumor cell growth.[35] The elevated expression of COX-2 is closely related to the enhancement of malignant transformation, which is in line with findings indicating the involvement of COX-2 in numerous malignancies including colon, breast, and lung cancer.[36] More recently, the potential role of COX-2 in leukemia and lymphoma pathogenesis has been reported. For instance, COX-2 reduces apoptosis and cellular attachment to the extracellular matrix. Increased levels of COX-2 and decreased progenitor adherence to bone marrow extracellular matrix have been observed in chronic myeloid leukemia.[37] The increased expression and activity of COX-2 in the pathogenesis of lymphoma has also been described in a recent study[38] and in leukemia cell lines by Nakanishi and colleagues.[39] These data are in line with another report showing that COX-2 overexpression represents a mechanism of resistance to apoptosis in B-chronic lymphoid leukemia and that pharmacological suppression of COX-2 might enhance chemotherapy-mediated apoptosis.[40,41] In addition, a number of recent reports have implicated COX-2 in the pathogenesis and resistance to therapy. In fact, one study demonstrated improved efficacy when the COX-2 inhibitor thalidomide was added in patients with multiple myeloma.[42]

Based on reports from the literature indicating that COX-2 as well as C/EBPβ play a critical role mediating resistance to apoptosis in response to AhR agonists, we have further characterized the putative role of C/EBPβ and COX-2 in regulating cell growth/apoptosis of various lymphoma cell types *in vitro* as well as a possible association with the development of lymphoma in a mouse model after treatment with TCDD.

Materials and Methods

Reagents

TCDD (>99% purity) was originally obtained from Dow Chemicals Co. (Midland, MI). Dimethyl sulfoxide and corn oil were obtained from Sigma (St. Louis, MO). NS-398 was obtained from Calbiochem (La Jolla, CA). 3′-Methoxy-4′-nitroflavone was a kind gift of Josef Abel (University of Dusseldorf, Dusseldorf, Germany). Other molecular biological reagents were purchased from Qiagen (Valencia, CA) and Roche (Indianapolis, IN).

Lymphoma Cell Lines

The histiocytic lymphoma cell line U937 was obtained from American Type Culture Collection (Manassas, VA) and the NHL cell line DOHH-2 from DSMZ (Braunschweig, Germany). The Burkitt lymphoma cell line Namalwa was a kind gift of E. McGrath (National Cancer Institute, National Institutes of Health, Bethesda, MD). Cells were maintained in RPMI 1640 medium containing 10% fetal bovine serum (Invitrogen, Carlsbad, CA), supplemented with 4.5 g/L glucose, 1 mmol/L sodium pyruvate, and 10 mmol/L HEPES without antibiotics. Cell culture was maintained at a cell concentration between 2×10^5 and 2×10^6 cells/ml.

Apoptosis Detection by Annexin V Staining

Cells were seeded at 1×10^4 cells in 12-well culture plates. After treatment for 72 hours with 10 nmol/L TCDD, apoptosis was induced by UV light (100 μJ/cm^2) for 1 minute. After 4 hours, cells were collected by centrifugation for 5 minutes at $350 \times g$. A total of 2×10^5 cells are resuspended in 50 μl of 1× annexin V binding buffer (10 mmol/L HEPES, pH 7.4, 140 mmol/L NaCl, and 2.5 mmol/L $CaCl_2$) supplemented with 5 μl of annexin V-fluorescein isothiocyanate (Sigma) and 5 μl of propidium iodide (PI) solution (50 μg/ml). The cells were gently mixed and incubated for 10 minutes at room temperature in the dark. Apoptotic cells were counted directly by using the fluorescence microscope (Leitz, Wetzlar, Germany). In each experiment, three representative aliquots per cell line are counted for analysis. Both annexin V-

positive and annexin V-PI-double-positive cells were considered to be apoptotic.

Transfection of siRNA

Transfection of siRNA into cells was performed via Nucleofector technology as described.[43] In brief, 10^6 cells were resuspended in 100 μl of Nucleofector Solution V (Amaxa GmbH, Köln, Germany) and nucleofected with 1.5 μg of the corresponding siRNA using program V-001, which is preprogrammed into the Nucleofector device (Amaxa). After nucleofection, the cells were immediately mixed with 500 μl of prewarmed RPMI 1640 medium and transferred into six-well plates containing 1.5 ml of RPMI 1640 medium per well. The reduction of the target RNA and protein was detected by quantitative real-time reverse transcriptase-polymerase chain reaction (RT-PCR) and Western blot. siRNA to target human AhR (catalog no. M-004990) was designed and synthesized by Dharmacon (Lafayette, CO). Validated siRNA to target human C/EBPβ (catalog no. SI00073619), human COX-2 (catalog no. 1027169), and a negative control siRNA (catalog no. 10272280) were synthesized by Qiagen. Individual siRNAs were capable of effectively (>75%) reducing mRNA expression (see Figure 4).

Quantitative Real-Time PCR

For preparation of total RNA from lymph nodes and spleen, the tissues were homogenized first in TRIzol using a TissueLyser (Qiagen). The RNA was extracted with chloroform and further purified with a highly pure RNA isolation kit (Qiagen). RNA extraction and cDNA synthesis were performed as previously described.[44] Quantitative detection of mouse and human glyceraldehyde-3-phosphate dehydrogenase (GAPDH), COX-2, C/EBPβ, and members of the Bcl-2 gene family was performed with a LightCycler Instrument (Roche Diagnostics, Mannheim, Germany) using the Fast Real-Time SYBR Green PCR Kit (Qiagen) according to the manufacturer's instructions. Primer sequences are listed in Table 1. DNA-free total RNA (0.01 to 1.0 μg) was reverse-transcribed using 4 U of Omniscript reverse transcriptase (Qiagen) and 1 μg of oligo(dT)$_{15}$ in a final volume of 40 μl. The primers for each gene were designed on the basis of the respective cDNA or mRNA sequences using OLIGO primer analysis software, provided by Steve Rosen and Whitehead Institute/Massachusetts Institute of Technology Center for Genome Research, Cambridge, MA. PCR amplification was performed in a total volume of 20 μl, containing 2 μl of cDNA, 10 μl of 2× Fast Real-Time SYBR Green PCR master mix, and 0.2 μmol/L of each primer. The PCR cycling conditions were 95°C for 5 minutes followed by two-step cycling 40 cycles of 95°C for 10 seconds, and 60°C for 30 seconds. Gene expression was quantified using an absolute standard curve method according to Leong and colleagues.[45] In brief, the single amplified PCR product was verified based on size in a 3% agarose gel under UV illumination. The gel band containing the DNA target was excised and digested to recover and purify the amplified product. The concentration of the amplified product was measured with a spectrophotometer. Using the average molecular weight of the product and Avogadro's constant, the number of copies per unit volume was calculated. The volume of the purified linear dsDNA standards was adjusted to 10^{10} copies per μl. This stock solution was serially diluted to obtain a standard series from 10^9 to 10 copies per μl with each step differing by 10-fold. When assaying the samples for the gene of interest, the corresponding standards series was run under the same conditions, and the copy numbers of samples was determined by reading off the standards series with the C_t values of the samples. Detection of the fluorescent product was performed at the end of the 60°C combined annealing/extension period. Negative controls were run concomitantly to confirm that the samples were not cross-contaminated. A sample with DNase- and RNase-free water instead of RNA was concomitantly examined for each of the reaction units described above. To confirm the amplification specificity, the PCR products were subjected to melting curve analysis. All PCR assays were performed in duplicate or triplicate. The intra-assay variability was <7%. For quantification, data were analyzed with the LightCycler analysis software according to the manufacturer's instructions.

Table 1. Sequences of Primers Used for Quantitative Real-Time PCR

Primer	Sequences
Human BAX	FP 5′-TTTGCTTCAGGGTTTCATCC-3′
	RP 5′-CAGTTGAAGTTGCCGTCAGA-3′
Human Bcl-2	FP 5′-CGGAGGATGAGTGACGAGTT-3′
	RP 5′-GATGTGGAGCGAAGGTCACT-3′
Human Bcl-w	FP 5′-GGACAAGTGCAGGAGTGGAT-3′
	RP 5′-GTCCTCACTGATGCCCAGTT-3′
Human Bcl-xl	FP 5′-TTGGACAATGGACTGGTTGA-3′
	RP 5′-GGGCCTCAGTCCTTTCTCTT-3′
Human C/EBPβ	FP 5′-GACAAGCACAGCGACGAGTA-3′
	RP 5′-AGCTGCTCCACCTTCTTCTG-3′
Human COX-2	FP 5′-TGAAACCCACTCCAAACACA-3′
	RP 5′-GAGAAGGCTTCCCAGCTTTT-3′
Human GAPDH	FP 5′-GAGTCAACGGATTTGGTCGT-3′
	RP 5′-TTGATTTTGGAGGGATCTCG-3′
Human Mcl-1	FP 5′-TGCTGGAGTAGGAGCTGGTT-3′
	RP 5′-CCTCTTGCCACTTGCTTTTC-3′
Mouse Bcl-xl	FP 5′-GCTGGGACACTTTTGTGGAT-3′
	RP 5′-TGTCTGGTCACTTCCGACTG-3′
Mouse C/EBPβ	FP 5′-GCGCGAGCGCAACAACATCT-3′
	RP 5′-TGCTTGAACAAGTTCCGCAG-3′
Mouse COX-2	FP 5′-AGAAGGAAATGGCTGCAGAA-3′
	RP 5′-GCTCGGCTTCCAGTATTGAG-3′
Mouse GAPDH	FP 5′-AACTTTGGCATTGTGGAAGG-3′
	RP 5′-ACACATTGGGGGTAGGAACA-3′

FP, forward primer; RP, reverse primer.

Western Blot Analysis

To analyze the level of intracellular COX-2 protein, whole-cell protein extracts (25 μg) were separated on a 10% sodium dodecyl sulfate-polyacrylamide gel and blotted onto a polyvinylidene difluoride membrane (Immuno-Blot; Bio-Rad, Hercules, CA). Blotted filters were blocked for 60 minutes in a 3% suspension of dried skimmed milk in

phosphate-buffered saline and incubated overnight at 4°C with a human COX-2-specific polyclonal antibody (Cayman Chemicals, Ann Arbor, MI). The antigen-antibody complexes were visualized using the chemiluminescence substrate SuperSignal, West Pico (Pierce, Rockford, IL) as recommended by the manufacturer. For quantitative analysis, respective bands were quantified using a ChemiImager4400 (Alpha Innotech Corp., San Leandro, CA).

Identification of Prostanoid Synthesis by Liquid Chromatography/Mass Spectrometry (LC/MS)

To obtain insights into the possible alteration of the synthesis of prostaglandins, which are involved in cellular processes including cell growth, differentiation, and apoptosis, LC/MS analyses was performed. Cell culture media of U937 cells was collected at various time points and spiked with internal standards and extracted as previously described.[46] After gentle base hydrolysis, extracts were separated by reversed phase high performance liquid chromatography and analyzed using negative mode electrospray ionization with a tandem mass spectral detector (Quattro Premiere; Micromass, Milford, MA) operated in multireaction monitoring mode. The analytical procedures remained essentially as published[46]; however, the mass spectral acquisition parameters have been modified to allow the simultaneous quantification of prostanoids; thromboxanes; lipoxins; hydroxyl-furans; ketones; epoxides; and mono-, di-, and tri-hydroxy metabolites of arachidonic and linoleic acids (>40 analytes).

Animals and Treatment

Female C57BL/10J mice were purchased from Jackson Laboratory (West Sacramento, CA). Mice were housed (four per cage) in a selective pathogen-free facility and humidity- and temperature-controlled room. The animals were maintained on a 12:12 hour-light/dark cycle and had free access to water and food according to the guidelines set by the University of California at Davis. Mice were allowed to adapt to the facility for 1 week. Each group consisted of four mice of 8-week-old female C57BL/10J mice fed on a regular diet. TCDD was prepared from a stock solution and diluted in corn oil. TCDD was administered via intraperitoneal injection. The control group received the vehicle corn oil (5 μl/g) alone, and the TCDD-treated group received an initial dose of 20 μg of TCDD/kg and a biweekly maintenance dose of 1 μg/kg TCDD throughout a period of 140 days.

[^{18}F]Fluorodeoxyglucose (FDG) Administration in Mice and Micropositron Emission Tomography Imaging

Development of lymphoma in C57BL/10J mice was monitored using microPET imaging. MicroPET imaging using FDG has become a useful imaging modality in the staging and treatment evaluation algorithm for lymphoma, providing unique metabolic information. All microPET imaging was conducted in the Center for Molecular and Genomic Imaging (CMGI) at University of California at Davis. PET images were acquired on a Siemens Focus 120 microPET system (Siemens, Knoxville, TN). Image analysis was performed using the accompanying ASIPro (Siemens) software.

Pathogen-free female C57BL/10J mice were anesthetized with isoflurane for the duration of the imaging study. The [^{18}F]FDG was injected as a bolus injection into the tail vein of the mouse. One hundred μCi of tracer was injected. The animal was positioned on a custom-built bed in the microPET II scanner. At the moment of radiotracer injection, data acquisition was initiated in list mode on the microPET II scanner. Imaging continued for a total time of 90 minutes. At the end of the study, the list mode data are binned into time frames as follows: 10 frames of 60 seconds, 10 frames of 120 seconds, and 12 frames of 300 seconds. Each frame will be reconstructed with a validated statistical three-dimensional reconstruction algorithm. Lymph nodes from control and TCDD-treated mice were removed for histopathological evaluation and extraction of total RNA.

Histopathology and Immunohistochemistry

At necropsy inguinal and axillary lymph nodes from TCDD-treated mice and controls were fixed in 10% formalin and then paraffin-embedded using standard histology protocols. Five-μm sections were cut and stained with hematoxylin and eosin, and further sections were used for immunohistochemistry. Immunohistochemical stains to detect CD3 and Pax-5 were performed to identify T- and B-lymphocyte populations, respectively. Briefly, endogenous peroxidase was blocked with 3% hydrogen peroxidase/methanol. Then the slides were incubated in fresh citrate buffer, pH 6.0, at 125°C for antigen retrieval. The primary antibodies were diluted in 0.5% phosphate-buffered saline and ovalbumin and incubated at room temperature overnight. Detection was performed using a biotinylated secondary antibody followed by the Avidin-Biotin-Peroxidase Complete ABC kit

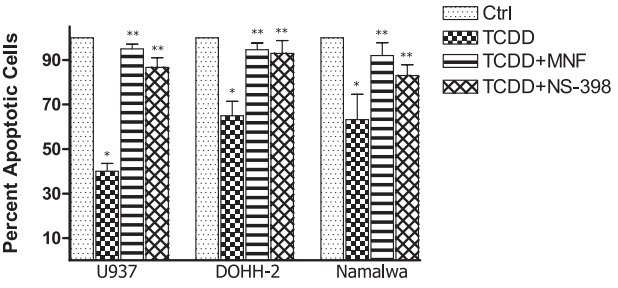

Figure 1. Effect of TCDD on UV-induced apoptosis in lymphoma cell lines. U937, Namalwa, and DOHH-2 cells were treated with 10 nmol/L TCDD for 48 hours. Then, apoptosis was induced by UV light, and the number of apoptotic cells was determined after 4 hours. Data are shown as percent inhibition versus control. In parallel experiments, cells were co-cultured with the COX-2 inhibitor NS-398 or the AhR antagonist 3′-methoxy-4′-nitroflavone. Data are means ± SD of results from three independent experiments performed. *Significantly different from control $P \leq 0.01$, and **significantly different from cells treated with TCDD alone $P \leq 0.01$.

Table 2. Expression of C/EBPβ, COX-2, and Bcl-xl in Various Human Lymphoma Cell Lines

Cell line	C/EBPβ	COX-2	Bcl-xl
U937	3.4 ± 1.4*	9.5 ± 2.1*	2.8 ± 0.3*
DOHH-2	2.5 ± 0.7*	4.7 ± 1.6*	2.1 ± 0.2*
Namalwa	1.8 ± 0.3*	2.2 ± 0.5*	1.7 ± 0.2*

U937, Namalwa, and DOHH-2 cells were treated with 10 nmol/L TCDD for 48 hours, and mRNA expression of C/EBPβ, COX-2, and Bcl-xl was analyzed by real-time PCR. These data are shown as fold induction relative to control cells (=1). Data are means ± SD of results from three independent experiments performed in duplicates.
* Significantly different from control $P \leq 0.01$.

(Vector Laboratories, Burlingame, CA) and developed with diaminobenzidine chromogen substrate.

Statistics

Data were analyzed by the paired Student's *t*-test and one-way analysis of variance as appropriate. If statistical significance ($P \leq 0.05$) was determined by analysis of variance, the data were further analyzed by Tukey's pairwise comparisons to detect specific differences between treatments.

Results

AhR-Mediated Inhibition of Apoptosis in Lymphoma Cell Lines Is COX-2-Dependent

Results in Figure 1 show that activation of AhR by TCDD significantly inhibits UV-induced apoptosis in the human lymphoma cell lines U937, DOHH-2, and Namalwa. The number of UV-induced apoptotic cells was reduced by 25, 35, and 60% in Namalwa, DOHH-2, and U937 cells, respectively, after treatment with 10 nmol/L TCDD for 48 hours (Figure 1). Next, we investigated, whether NS-398 is able to abolish the TCDD-mediated inhibition of apoptosis. The chemoprotective effect of the COX-2 inhibitor NS-398 eliminated the anti-apoptotic effect of TCDD by ~80 to 95% *in vitro*. The AhR antagonist 3′-methoxy-4′-nitroflavone abolished the anti-apoptotic effect of TCDD significantly by ~90% (Figure 1). The anti-apoptotic effect of TCDD coincided with an increased expression of C/EBPβ, COX-2, and Bcl-xl in all three lymphoma cell lines tested (Table 2). The effect of TCDD on apoptosis and expression of COX-2 was most significant in U937 cells. Therefore, U937 cells were used for further mechanistic studies. Suppression of AhR by gene silencing abolished the anti-apoptotic effect of TCDD by more than 90%. Suppression of C/EBPβ or COX-2 by siRNA led to a decrease of ~60% of the TCDD-mediated inhibition of apoptosis (Figure 2). The results with gene silencing support that the TCDD-mediated anti-apoptotic effects are AhR-dependent and involve the transcription factor C/EBPβ as well as the activity of COX-2.

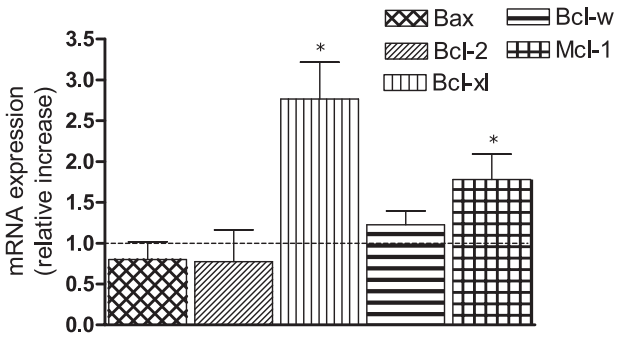

Figure 3. Treatment of the U937 lymphoma cell line with TCDD results in increased levels of Bcl-xl and Mcl-1 mRNA levels. Cells were treated with 10 nmol/L TCDD for 48 hours, and mRNA expression of Bax, Bcl-2, Bcl-w, Bcl-xl, and Mcl-1 was analyzed by real-time PCR. These data are shown as fold induction relative to control cells. Data are means ± SD of results from three independent experiments performed in duplicates. *Significantly different from control $P \leq 0.01$.

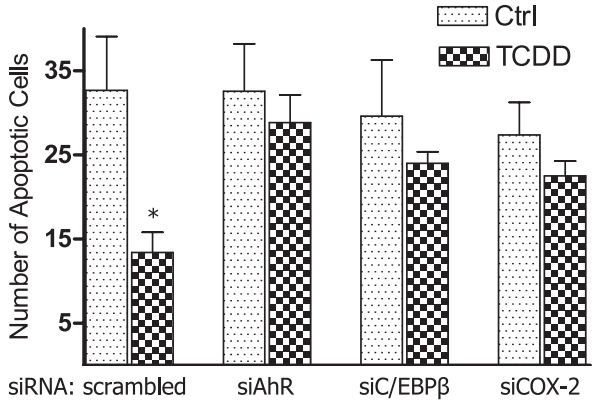

Figure 2. Effect of AhR, C/EBPβ, and COX-2 gene silencing on TCDD-mediated apoptotic resistance in U937 cells. Cells were pretreated with TCDD or dimethyl sulfoxide (control) before apoptosis was induced by UV light. To block the TCDD- and AhR-mediated effect on apoptosis U937 cells were transfected with siRNA specific for AhR, C/EBPβ, or COX-2 for 24 hours before cells were treated with TCDD for 48 hours. Then, apoptosis was induced by UV light, and the number of apoptotic cells was determined after 4 hours. Values are averages of duplicates from two different experiments. *Significantly different from control $P \leq 0.01$.

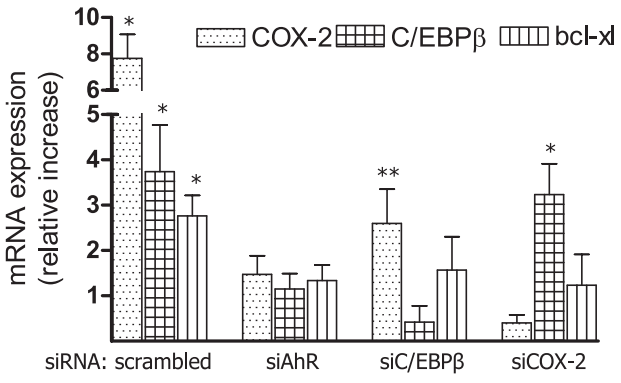

Figure 4. Induction of C/EBPβ and COX-2 by TCDD is AhR-dependent. To block the TCDD-induced expression of COX-2, C/EBPβ, and Bcl-xl, U937 cells were transfected with siRNA specific for AhR, C/EBPβ, or COX-2 for 24 hours before cells were treated with TCDD for 48 hours. Data are means ± SD of results from three independent experiments. *Significantly increased compared with control $P \leq 0.01$, and **significantly decreased compared with control $P \leq 0.01$.

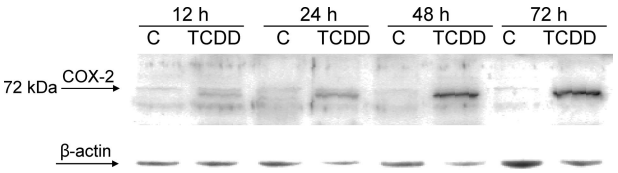

Figure 5. Time-dependent increased level of COX-2 protein in U937 cells treated with TCDD. Whole cell lysates from the U937 lymphoma cell line were prepared after treatment with 10 nmol/L TCDD for 12, 24, 48, and 72 hours and analyzed by immunoblotting using a polyclonal human COX-2-specific antibody. A representative result of three independent experiments is shown.

Effect of TCDD on Bcl-2 Proto-Oncogenes

The Bcl-2 proto-oncogene family of proteins has been found to be important in regulating apoptosis in B cells and is involved in the pathogenesis of several subtypes of B-cell lymphomas.[47] These proteins include the anti-apoptotic proteins Bcl-2, Mcl-1, and Bcl-xl, and the pro-apoptotic protein Bax. Levels of Bcl-2, Bcl-xl, Mcl-1, and Bax mRNA were examined by real-time PCR. The levels of Bcl-2 and the proapoptotic Bax were slightly decreased within the 48 hours of treatment with TCDD compared with control (Figure 3). However, the anti-apoptotic proteins Bcl-xl as well as Mcl-1 were significantly increased by TCDD in U937 cells.

Increase of COX-2 Is AhR- and C/EBPβ-Dependent and Involves Induction of Bcl-xl

To investigate whether the TCDD-mediated increase of COX-2 is AhR-dependent and mediated through C/EBPβ as described earlier,[44] we analyzed the expression of COX-2, C/EBPβ, and Bcl-xl in U937 cells transfected with siRNA targeting the AhR, C/EBPβ, and COX-2. After 72 hours of siRNA transfection, the targeted mRNA was down-regulated by at least 70%. The results in Figure 4 show that treatment with TCDD for 48 hours induces COX-2, C/EBPβ, and Bcl-xl in an AhR-dependent manner. Using the linear DNA standards method, the absolute amount of mRNA was calculated as 1.4×10^4 copies of COX-2, 5.5×10^6 copies of C/EBPβ, and 5.0×10^6 copies of Bcl-xl per 10 ng of total RNA of control U937 cells. The TCDD-induced levels of COX-2 and Bcl-xl mRNA were significantly suppressed by transfection with C/EBPβ-specific siRNA. Transfection with siRNA targeting COX-2 led to a significant reduction of Bcl-xl mRNA but did not significantly affect the expression of C/EBPβ (Figure 4).

COX-2 Induction Is Associated with a Time-Dependent Increase of COX-2 Protein and Secretion of PGE_2, $PGF_{2\alpha}$, and TBX_2

As shown in Figure 5, the induction of COX-2 mRNA correlates with a time-dependent increase of COX-2 protein. A first significant increase of COX-2 protein was observed after 24 hours of TCDD treatment, which was further elevated after 48 and 72 hours of treatment (Figure 5). To investigate possible alterations of the synthesis of prostanoids caused by increased COX-2 expression, we quantified ~40 metabolites of arachidonic acid (AA) and linoleic acids by LC/MS analysis. Table 3 shows that levels of three COX-2-dependent AA metabolites including prostaglandin E_2 (PGE_2), prostaglandin $F_{2\alpha}$ ($PGF_{2\alpha}$), and thromboxane B_2 (TBX_2) in supernatant of U937 cells were time dependently increased by treatment with TCDD throughout a time period of 72 hours. Of the 40 different AA metabolites measured by LC/MS, only the level of PGE_2, $PGF_{2\alpha}$, and TBX_2 was significantly affected by treatment with TCDD (Table 3). The most significant increase of 3- to 10-fold after 48 and 72 hours, respectively, by TCDD was found for PGE_2, which is in line with a previous study.[33] The level of $PGF_{2\alpha}$ and TBX_2 was approximately twofold elevated at 72 hours after TCDD treatment.

Studies on the Effect of TCDD on Lymphoma Development in C57BL/10J Mice

This project was started by testing the effect of TCDD in two groups: C57BL/10J vehicle control (corn oil) intraperitoneally and intraperitoneal injection of an initial dose of 20 μg of TCDD/kg. Mice received a biweekly maintenance dose of 1 μg of TCDD/kg intraperitoneally. Each group consisted of three 8-week-old female C57BL/10J mice fed on regular diet. To assess tumor development mice were scanned for the first time after 30 days of initial treatment with TCDD by microPET imaging using FDG. A second PET imaging was performed 60 days after initial

Table 3. Effect of TCDD on the Production of Prostanoids

	Prostanoid levels (pg/mg protein)					
	PGE_2		$PGF_{2\alpha}$		TBX_2	
Time	Control	TCDD	Control	TCDD	Control	TCDD
0 hours	68 ± 8	73 ± 3	383 ± 23	370 ± 13	657 ± 12	602 ± 9
12 hours	109 ± 22	138 ± 10	256 ± 20	275 ± 19	597 ± 25	631 ± 16
24 hours	68 ± 9	143 ± 11*	309 ± 9	350 ± 11*	720 ± 27	798 ± 20*
48 hours	59 ± 7	214 ± 14*	349 ± 10	464 ± 22*	778 ± 19	802 ± 31*
72 hours	53 ± 4	503 ± 21*	366 ± 8	890 ± 45*	732 ± 12	1411 ± 56*

Arachidonic acid metabolites, including prostaglandin E_2 (PGE_2), prostaglandin $F_{2\alpha}$ ($PGF_{2\alpha}$), and thromboxane B_2 (TBX_2), in supernatant of U937 cells treated for 12, 24, 48, and 72 hours with 10 nmol/L TCDD were measured by LC/MS. Results of triplicates are presented as means ± SD.
*Significantly different from control $P \leq 0.01$.

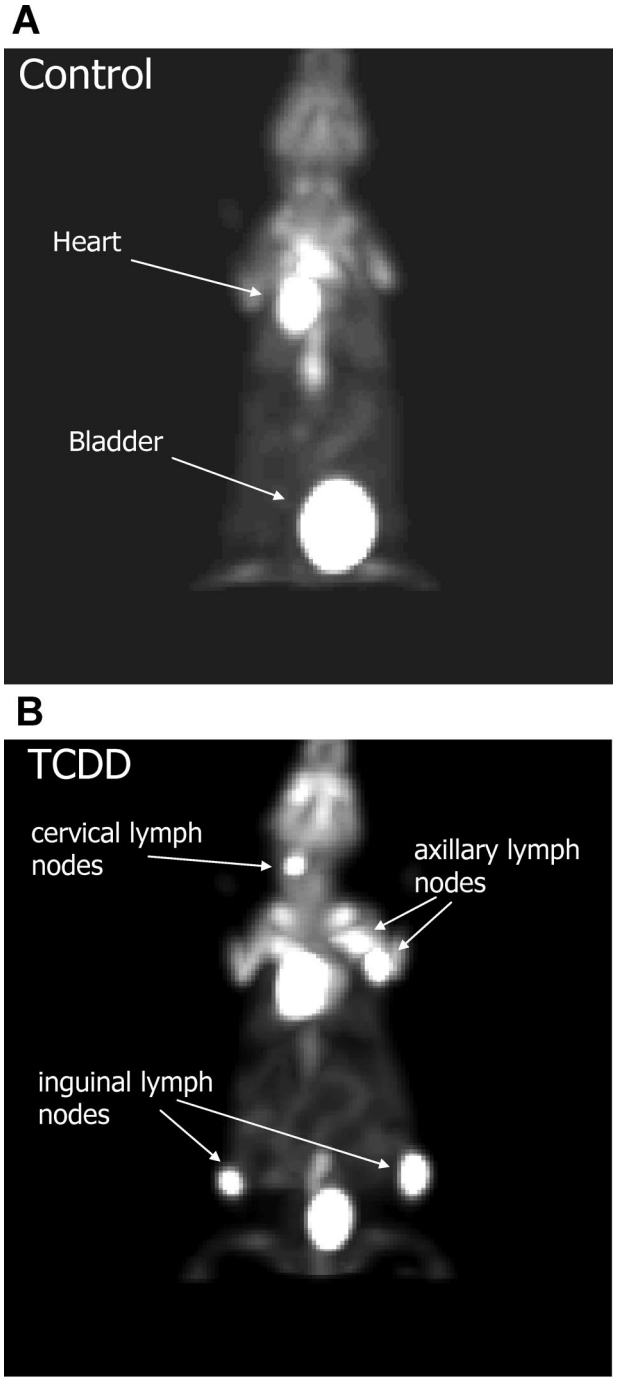

treatment. No visible signs of lymphoma development could be observed in control or TCDD-treated animals at the time of the first two PET scans 30 or 60 days after initial treatment (data not shown). One hundred-forty days after the initial treatment, a third PET imaging revealed activity consistent with lymphoma development in the TCDD-treated animals (Figure 6A), whereas control animals showed no signs of tumor development at this time point (Figure 6B). These results were confirmed in a second independent experiment with four animals in each group demonstrating FDG uptake consistent with the development of lymphoma only in TCDD-treated animals after 140 days of treatment. Activity in the heart and bladder caused by normal accumulation of FDG is usually detectable in all mice (Figure 6, A and B). The distinct anatomical location of the increased FDG activity is indicative of lymphomatous development. According to the localization, they are classified as superficial cervical lymph nodes, situated immediately above the submandibular salivary glands; axillary lymph nodes, present in the axillary fossa, and inguinal lymph nodes situated close to the bifurcation of the superficial epigastric vein (Figure 6B). Animals were sacrificed to remove lymph nodes and spleens to examine further the expression of COX-2, C/EBPβ, and Bcl-xl, as well as pathological evaluation for confirmation of lymphomatous development. In line with results from *in vitro* studies, we found a clear increase of COX-2 (17-fold), as well as significantly elevated levels of C/EBPβ and Bcl-xl in the inguinal and axillary lymph nodes of TCDD-treated animals compared with lymph nodes of control animals. The absolute amount of mRNA was calculated as 0.6×10^4 copies of COX-2, 1.5×10^6 copies of C/EBPβ, and 1.2×10^6 copies of Bcl-xl per 10 ng of total RNA of inguinal lymph nodes derived from control mice. A moderate increase for COX-2 and C/EBPβ of approximately twofold was found in spleen of TCDD-treated animals (Figure 6C).

Histopathology Findings

Inguinal and axillary lymph nodes from TCDD-treated mice and controls were removed at necropsy. Both axillary and inguinal lymph nodes were enlarged (four to six times the size of the control lymph nodes), as a result of marked expansion of the cortex in B-cell zones (Figure 7, A and B). Within the medullary sinusoids there was infiltration of histiocytes and plasma cells intermingled with rare neutrophils. The cells in the expanded regions of the

Figure 6. Development of lymphomas in axillary and inguinal lymph nodes of TCDD-treated C57BL/10J mice is associated with overexpression of COX-2. **A** and **B:** MicroPET imaging of control (**A**) and TCDD-treated (**B**) C57BL/10J mice using [^{18}F]fluorodeoxyglucose (FDG). Mice received an initial dose of 20 μg of TCDD/kg b.wt. and a biweekly maintenance dose as described in Materials and Methods. Control mice received the corresponding amount of corn oil. MicroPET imaging was taken 140 days after initial treatment. **C:** Increased expression level of COX-2, C/EBPβ, and Bcl-xl mRNA in lymphoma tissue of TCDD-treated C57BL/10J mice. RNA was isolated from fresh lymph nodes and spleen 140 days after initial treatment and analyzed by real-time PCR. The induced mRNA expression is given relative to the values of control animals. Data are means ± SD of results from three animals of each group. *Significantly different from control $P \leq 0.05$.

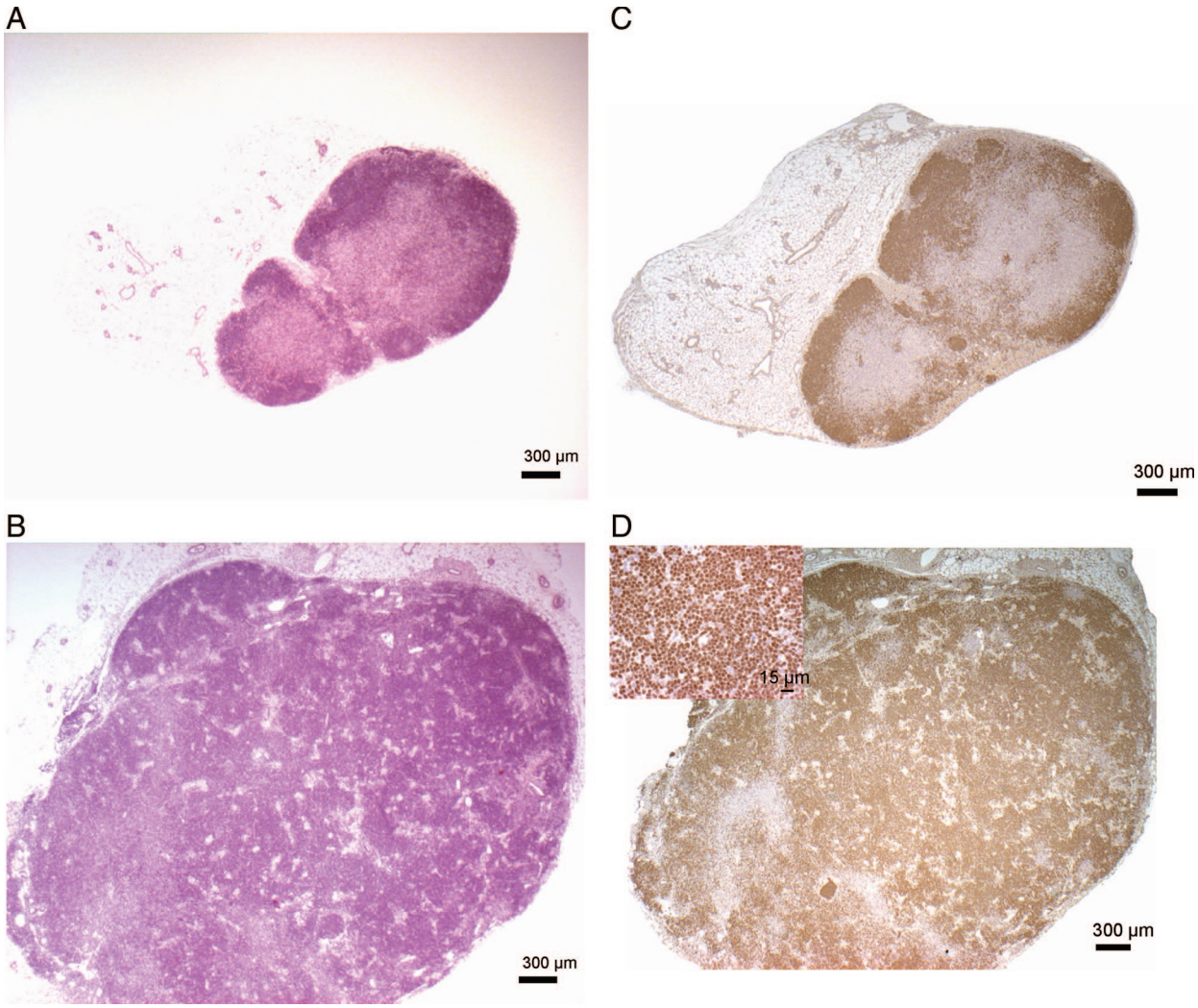

Figure 7. H&E staining and expression of the B-cell marker Pax5 in lymph node biopsies. Biopsies from lymph nodes of C57BL/10J mice were analyzed using H&E staining and by immunohistochemistry. **A:** H&E-stained lymph node from control mouse. **B:** H&E-stained lymph node from TCDD-treated mouse. **C:** Pax5 expression in lymph node from control mouse. **D:** Pax5 expression in lymph node from TCDD-treated mice. **Inset** depicts strong positive staining for Pax5. A representative sample is shown. Scale bar = 300 μm. Original magnifications: ×25 (**A–D**); ×500 (**D**, **inset**).

cortex were characterized by tightly packed sheets of small lymphocytes, which still respected the architecture of the lymph node and stained strongly with Pax5, a B-cell marker (Figure 7, C and D). The Pax5 gene encodes the B-cell lineage-specific activator protein (BSAP) that is expressed at early, but not late, stages of B-cell differentiation. Pax5 has also been implicated in human B-cell malignancies because it is deregulated by chromosomal translocations in a subset of acute lymphoblastic leukemias and NHL.[48] None of the lymphocytes in the expanded regions stained with CD3, a T-cell marker (data not shown). These features are consistent with a lymphoproliferative disorder indicating a premalignant state in the lymph nodes.

Discussion

This study shows that activation of the AhR results in resistance to an apoptotic response in three different human lymphoma cell lines. Previous reports have shown that the ligand-dependent activation of AhR by TCDD leads to inhibition of apoptosis *in vitro* as well as *in vivo*.[20–25] Consequently, the anti-apoptotic response has been linked to the tumor-promoting action of TCDD and other dioxin-like compounds that activate the AhR.[18,23] The anti-apoptotic effect observed in this study correlates with the TCDD-induced expression of COX-2, C/EBPβ, and Bcl-xl in U937, DOHH-2, and Namalwa cells. Suppression of AhR and COX-2 using gene-silencing technique and specific inhibitors indicate that the anti-apoptotic effect of TCDD is mediated through the AhR and COX-2 signaling pathway. The results further show that the induction of COX-2 as well as Bcl-xl involves the expression of C/EBPβ. These data are in line with recent findings showing that the AhR-mediated induction of COX-2 by TCDD involves the stimulation of C/EBPβ signaling.[33,44] Like COX-2, C/EBPβ is known to contribute to the deregulation of Bcl-2 and apoptosis in lymphoma cells.[27] The AhR-dependent induction of COX-2 by TCDD has been shown previously in multiple cell lines as well as

in vivo.[49,50] Although the increased expression of COX-2 is consistent in lymphoma cell lines and high levels of prostaglandins have been found in patients with lymphoma,[40,51] the role of COX-2 in the pathogenesis of lymphoma is not well defined. However, COX-2 is a likely candidate mediating the anti-apoptotic effect of the TCDD-activated AhR because overexpression of COX-2 has been shown to result in increased resistance to apoptosis.[52] The role of COX-2 in preventing apoptosis is obviously mediated by COX-2-derived PGE_2, which attenuates cell death.[53] One of the downstream targets of PGE_2 responsible for the anti-apoptotic effect seems to be the increased expression of members of the Bcl-2 family including Bcl-xl and Mcl-1,[53,54] which may be a key anti-apoptotic mediator. The only other COX-2-derived prostaglandin implicated in oncogenesis is TXA_2, which was reported to promote angiogenesis.[55] To obtain insights into the possible alteration of the synthesis of prostaglandins, which are involved in cellular processes including cell growth, differentiation, and apoptosis, LC/MS analyses was performed. In the current study, we could show that the time-dependent increase of COX-2 protein results in distinct elevated levels of PGE_2 secreted by U937 cells treated with TCDD. Therefore, it seems reasonable that the COX-dependent inhibition of apoptosis by TCDD is attributable to increased levels of $PGE_{2,}$ which may mediate the increased expression of Bcl-xl and Mcl-1. The ability of Bcl-2 proto-oncogenes to inhibit apoptosis is well accepted. Several members of the Bcl-2 gene family have also been identified including Bcl-2, Bcl-w, Bcl-xL, and Mcl-1, which function as repressors of apoptosis.[47] The level of Bcl-2 or Bcl-w did not significantly change in U937 cells by TCDD, whereas Mcl-1 was increased. The most significant effect has been observed on the expression of Bcl-xL, which was increased by TCDD in all three lymphoma cell lines included in this study.

The most important question we addressed was whether TCDD would indeed promote the development of lymphoma *in vivo*. In an effort to find evidence for the promoting effect of TCDD on the development of lymphoma in an animal model, we chose the C57BL/10J mouse. C57BL/10J is a substrain of C57BL/6J, which is a widely used inbred strain expressing the b-allele for a high-affinity AhR. MicroPET imaging revealed lymphoma development in animals after 140 days of the initial treatment with TCDD, whereas control animals showed no signs of tumor development at this time point. Distinct foci of increased activity in the TCDD-treated animals occur at anatomical locations consistent with lymphomatous involvement, for example the axillary and inguinal lymph nodes. Malignant lymphomas could not be diagnosed by histopathological evaluation, but increased lymphoproliferation was evident indicating a premalignant state of the lymph node. To investigate the most prominent effects of the *in vitro* studies, we analyzed the expression of COX-2, C/EBPβ, and Bcl-xL in the lymphoma tissues. In line with results from *in vitro* studies, we found a clear increase of COX-2 as well as significantly elevated expression levels of C/EBPβ and Bcl-xL in the inguinal and axillary lymph nodes of TCDD-treated animals compared with lymph nodes of control animals. To evaluate the absolute amount of mRNA transcripts, a linear DNA standards method was used. The results revealed that the abundances of COX-2 as well as Bcl-xl mRNAs in U937 cells are similar compared with the amount of the corresponding mRNA transcripts found in inguinal lymph nodes of mice. These data suggest that the amount of COX-2 mRNA induced by TCDD for instance is likely to be sufficient to exert a biological effect, which is supported by the analysis of COX-2 protein and the level of PGE_2 determined in U937 cells.

Taken together, the results indicate that TCDD provides a favorable environment for tumor transformation through up-regulation of COX-2, C/EBPβ, and Bcl-xL because histopathology findings demonstrate a premalignant state of the lymph nodes at this time point. Further, this study showed that the activity of AhR and COX-2 are critical factors inducing a resistance of the apoptotic response in lymphoma cell lines and the development of lymphoma *in vivo*. These findings indicate that AhR antagonists might be a useful approach to enhance pro-apoptotic actions of cancer therapies. To determine the relevance of the AhR activation and COX-2 overexpression, further *in vivo* studies are needed to investigate the potential chemopreventive effect of AhR antagonists and COX-2 inhibitors on the development of lymphoma.

Acknowledgments

We thank Katherine Wasson, Chris Griesemer, Lisa Dillard-Telm, Jennifer Fung, and Steve Rending for their excellent technical support.

References

1. Titcomb Jr CP: Non-Hodgkin's lymphoma: in a class all its own. J Insur Med 2001, 4:329–338
2. Clarke CA, Glaser SL: Changing incidence of non-Hodgkin lymphomas in the United States. Cancer 2002, 94:2015–2023
3. Remontet L, Esteve J, Bouvier AM, Grosclaude P, Launoy G, Menegoz F, Exbrayat C, Tretare B, Carli PM, Guizard AV, Troussard X, Bercelli P, Colonna M, Halna JM, Hedelin G, Mace-Lesec'h J, Peng J, Buemi A, Velten M, Jougla E, Arveux P, Le Bodic L, Michel E, Sauvage M, Schvartz C, Faivre J: Cancer incidence and mortality in France over the period 1978–2000. Rev Epidemiol Sante Publique 2003, 51:3–30
4. Hardell L, Eriksson M, Nordstrom M: Exposure to pesticides as risk factor for non-Hodgkin's lymphoma and hairy cell leukemia: pooled analysis of two Swedish case-control studies. Leuk Lymphoma 2002, 43:1043–1051
5. Miligi L, Costantini AS, Bolejack V, Veraldi A, Benvenuti A, Nanni O, Ramazzotti V, Tumino R, Stagnaro E, Rodella S, Fontana A, Vindigni C, Vineis P: Non-Hodgkin's lymphoma, leukemia, and exposures in agriculture: results from the Italian multicenter case-control study. Am J Ind Med 2003, 44:627–636
6. Quintana PJ, Delfino RJ, Korrick S, Ziogas A, Kutz FW, Jones EL, Laden F, Garshick E: Adipose tissue levels of organochlorine pesticides and polychlorinated biphenyls and risk of non-Hodgkin's lymphoma. Environ Health Perspect 2004, 112:854–861
7. Zheng T, Blair A, Zhang Y, Weisenburger DD, Zahm SH: Occupation and risk of non-Hodgkin's lymphoma and chronic lymphocytic leukemia. J Occup Environ Med 2002, 44:469–474
8. Fingerhut MA, Halperin WE, Marlow DA: Cancer mortality in workers exposed to 2,3,7,8-tetrachlorodibenzo-p-dioxin. N Engl J Med 1991, 324:212–218
9. Bertazzi PA, Consonni D, Bachetti S: Health effects of dioxin exposure: a 20-year mortality study. Am J Epidemiol 2001, 153:1031–1044

10. Becher H, Flesch-Janys D, Kauppinen T, Kogevinas M, Steindorf K, Manz A, Wahrendorf J: Cancer mortality in German male workers exposed to phenoxy herbicides and dioxins. Cancer Causes Control 1996, 7:312–321
11. Hooiveld M, Heederik DJ, Kogevinas M, Boffetta P, Needham LL, Patterson Jr DG, Bueno-de-Mesquita HB: Second follow-up of a Dutch cohort occupationally exposed to phenoxy herbicides, chlorophenols, and contaminants. Am J Epidemiol 1998, 147:891–901
12. Flesch-Janys D, Steindorf K, Gurn P, Becher H: Estimation of the cumulated exposure to polychlorinated dibenzo-p-dioxins/furans and standardized mortality ratio analysis of cancer mortality by dose in an occupationally exposed cohort. Environ Health Perspect 1998, 106(Suppl 2):655–662
13. Viel JF, Arveux P, Baverel J, Cahn JY: Soft-tissue sarcoma and non-Hodgkin's lymphoma clusters around a municipal solid waste incinerator with high dioxin emission levels. Am J Epidemiol 2000, 152:13–19
14. IARC Working Group on the Evaluation of Carcinogenic Risks to Humans: Polychlorinated dibenzo-para-dioxins and polychlorinated dibenzofurans. Lyon, France, 4–11 February 1997. IARC Monogr Eval Carcinog Risks Hum 1997, 69:1–631
15. Yoon BI, Hirabayashi Y, Kawasaki Y, Kodama Y, Kaneko T, Kanno J, Kim DY, Fujii-Kuriyama Y, Inoue T: Aryl hydrocarbon receptor mediates benzene-induced hematotoxicity. Toxicol Sci 2002, 70:150–156
16. Hayashibara T, Yamada Y, Mori N, Harasawa H, Tsuruda K, Sugahara K, Miyanishi T, Kamihira S, Tomonaga M, Maita T: Possible involvement of aryl hydrocarbon receptor (AhR) in adult T-cell leukemia (ATL) leukemogenesis: constitutive activation of AhR in ATL. Biochem Biophys Res Commun 2003, 300:128–134
17. Komura K, Hayashi S, Makino I, Poellinger L, Tanaka H: Aryl hydrocarbon receptor/dioxin receptor in human monocytes and macrophages. Mol Cell Biochem 2001, 226:107–118
18. Luebeck EG, Buchmann A, Stinchcombe S, Moolgavkar SH, Schwarz M: Effects of 2,3,7,8-tetrachlorodibenzo-p-dioxin on initiation and promotion of GST-P-positive foci in rat liver: a quantitative analysis of experimental data using a stochastic model. Toxicol Appl Pharmacol 2000, 167:63–73
19. Schwarz M, Buchmann A, Stinchcombe S, Kalkuhl A, Bock K: Ah receptor ligands and tumor promotion: survival of neoplastic cells. Toxicol Lett 2000, 113:69–77
20. Schrenk D, Schmitz HJ, Bohnenberger S, Wagner B, Worner W: Tumor promoters as inhibitors of apoptosis in rat hepatocytes. Toxicol Lett 2004, 149:43–50
21. Wu R, Zhang L, Hoagland MS, Swanson HI: Lack of the aryl hydrocarbon receptor leads to impaired activation of AKT/protein kinase B and enhanced sensitivity to apoptosis induced via the intrinsic pathway. J Pharmacol Exp Ther 2007, 320:448–457
22. Ray SS, Swanson HI: Dioxin-induced immortalization of normal human keratinocytes and silencing of p53 and p16INK4a. J Biol Chem 2004, 279:27187–27193
23. Stinchcombe S, Buchmann A, Bock KW, Schwarz M: Inhibition of apoptosis during 2,3,7,8-tetrachlorodibenzo-p-dioxin-mediated tumour promotion in rat liver. Carcinogenesis 1995, 16:1271–1275
24. Davis JW Jr, Burdick AD, Lauer FT, Burchiel SW: The aryl hydrocarbon receptor antagonist, 3′methoxy-4′nitroflavone, attenuates 2,3,7,8-tetrachlorodibenzo-p-dioxin-dependent regulation of growth factor signaling and apoptosis in the MCF-10A cell line. Toxicol Appl Pharmacol 2003, 188:42–49
25. Park S, Matsumura F: Characterization of anti-apoptotic action of TCDD as a defensive cellular stress response reaction against the cell damaging action of ultra-violet irradiation in an immortalized normal human mammary epithelial cell line, MCF10A. Toxicology 2006, 217:139–146
26. Wessells J, Yakar S, Johnson PF: Critical prosurvival roles for C/EBP beta and insulin-like growth factor I in macrophage tumor cells. Mol Cell Biol 2004, 24:3238–3250
27. Heckman CA, Wheeler MA, Boxer LM: Regulation of Bcl-2 expression by C/EBP in t(14;18) lymphoma cells. Oncogene 2003, 22:7891–7899
28. Bundy LM, Sealy L: CCAAT/enhancer binding protein beta (C/EBP-beta)-2 transforms normal mammary epithelial cells and induces epithelial to mesenchymal transition in culture. Oncogene 2003, 22:869–883
29. Zhu S, Yoon K, Sterneck E, Johnson PF, Smart RC: CCAAT/enhancer binding protein-beta is a mediator of keratinocyte survival and skin tumorigenesis involving oncogenic Ras signaling. Proc Natl Acad Sci USA 2002, 99:207–212
30. Sterneck E, Zhu S, Ramirez A, Jorcano JL, Smart RC: Conditional ablation of C/EBPbeta demonstrates its keratinocyte-specific requirement for cell survival and mouse skin tumorigenesis. Oncogene 2006, 25:1272–1276
31. Wu KK, Liou JY, Cieslik K: Transcriptional control of COX-2 via C/EBPbeta. Arterioscler Thromb Vasc Biol 2005, 25:679–685
32. Vogel C: Prostaglandin H synthases and their importance in chemical toxicity. Curr Drug Metab 2000, 1:391–404
33. Vogel C, Boerboom AM, Baechle C, El-Bahay C, Kahl R, Degen GH, Abel J: Regulation of prostaglandin endoperoxide H synthase-2 induction by dioxin in rat hepatocytes: possible c-Src-mediated pathway. Carcinogenesis 2000, 21:2267–2274
34. Herschman HR: Prostaglandin synthase 2. Biochim Biophys Acta 1996, 1299:125–140
35. Lin MT, Lee RC, Yang PC, Ho FM, Kuo ML: Cyclooxygenase-2 inducing Mcl-1-dependent survival mechanism in human lung adenocarcinoma CL1.0 cells. Involvement of phosphatidylinositol 3-kinase/Akt pathway. J Biol Chem 2001, 276:48997–49002
36. Hawk ET, Viner JL, Dannenberg A, DuBois RN: COX-2 in cancer—a player that's defining the rules. J Natl Cancer Inst 2002, 94:545–546
37. Giles FJ, Kantarjian HM, Bekele BN, Cortes JE, Faderl S, Thomas DA, Manshouri T, Rogers A, Keating MJ, Talpaz M, O'Brien S, Albitar M: Bone marrow cyclooxygenase-2 levels are elevated in chronic-phase chronic myeloid leukaemia and are associated with reduced survival. Br J Haematol 2002, 119:38–45
38. Wun T, McKnight H, Tuscano JM: Increased cyclooxygenase-2 (COX-2): a potential role in the pathogenesis of lymphoma. Leuk Res 2004, 28:179–190
39. Nakanishi Y, Kamijo R, Takizawa K, Hatori M, Nagumo M: Inhibitors of cyclooxygenase-2 (COX-2) suppressed the proliferation and differentiation of human leukaemia cell lines. Eur J Cancer 2001, 37:1570–1580
40. Secchiero P, Barbarotto E, Gonelli A, Tiribelli M, Zerbinati C, Celeghini C, Agostinelli C, Pileri SA, Zauli G: Potential pathogenetic implications of cyclooxygenase-2 overexpression in B chronic lymphoid leukemia cells. Am J Pathol 2005, 167:1599–1607
41. Petlickovski A, Laurenti L, Li X, Marietti S, Chiusolo P, Sica S, Leone G, Efremov DG: Sustained signaling through the B-cell receptor induces Mcl-1 and promotes survival of chronic lymphocytic leukemia B cells. Blood 2005, 105:4820–4827
42. Prince HM, Mileshkin L, Roberts A, Ganju V, Underhill C, Catalano J, Bell R, Seymour JF, Westerman D, Simmons PJ, Lillie K, Milner AD, Iulio JD, Zeldis JB, Ramsay RA: Multicenter phase II trial of thalidomide and celecoxib for patients with relapsed and refractory multiple myeloma. Clin Cancer Res 2005, 11:5504–5514
43. Matsumura F, Vogel CF: Evidence supporting the hypothesis that one of the main functions of the aryl hydrocarbon receptor is mediation of cell stress responses. Biol Chem 2006, 387:1189–1194
44. Vogel CF, Sciullo E, Park S, Liedtke C, Trautwein C, Matsumura F: Dioxin increases C/EBPβ transcription by activating cAMP/protein kinase A. J Biol Chem 2004, 279:8886–8894
45. Leong DT, Gupta A, Bai HF, Wan G, Yoong LF, Too HP, Chew FT, Hutmacher DW: Absolute quantification of gene expression in biomaterials research using real-time PCR. Biomaterials 2007, 28:203–210
46. Newman JW, Watanabe T, Hammock BD: The simultaneous quantification of cytochrome P450 dependent linoleate and arachidonate metabolites in urine by HPLC-MS/MS. J Lipid Res 2002, 43:1563–1578
47. Cory S: Regulation of lymphocyte survival by the bcl-2 gene family. Annu Rev Immunol 1995, 13:513–543
48. Cobaleda C, Schebesta A, Delogu A, Busslinger M: Pax5: the guardian of B cell identity and function. Nat Immunol 2007, 8:463–470
49. Wolfle D, Marotzki S, Dartsch D, Schafer W, Marquardt H: Induction of cyclooxygenase expression and enhancement of malignant cell transformation by 2,3,7,8-tetrachlorodibenzo-p-dioxin. Carcinogenesis 2000, 1:15–21
50. Vogel C, Schuhmacher US, Degen GH, Bolt HM, Pineau T, Abel J: Modulation of prostaglandin H synthase-2 mRNA expression by 2,3,7,8-tetrachlorodibenzo-p-dioxin in mice. Arch Biochem Biophys 1998, 351:265–271
51. Sébahoun G, Maraninchi D, Carcassonne Y: Increased prostaglandin E production in malignant lymphomas. Acta Haematol 1985, 74:132–136

52. Tsujii M, DuBois RN: Alterations in cellular adhesion and apoptosis in epithelial cells overexpressing prostaglandin endoperoxide synthase 2. Cell 1995, 83:493–501
53. Sheng H, Shao J, Morrow JD, Beauchamp RD, DuBois RN: Modulation of apoptosis and Bcl-2 expression by prostaglandin E2 in human colon cancer cells. Cancer Res 1998, 58:362–366
54. Kataoka K, Takikawa Y, Lin SD, Suzuki K: Prostaglandin E2 receptor EP4 agonist induces Bcl-xL and independently activates proliferation signals in mouse primary hepatocytes. J Gastroenterol 2005, 40:610–616
55. Pradono P, Tazawa R, Maemondo M, Tanaka M, Usui K, Saijo Y, Hagiwara K, Nukiwa T: Gene transfer of thromboxane A(2) synthase and prostaglandin I(2) synthase antithetically altered tumor angiogenesis and tumor growth. Cancer Res 2002, 62:63–66